ISSN: 2641-1784

Research Article

Advance in Environmental Waste Management & Recycling

Comprehensive analysis of PCM container construction effects PV panels thermal management

H. Metwally[a]*, N. A. Mahmoud[a], W. Aboelsoud[a], M. Ezzat[b]

[a]*Power Mechanical Engineering*

[b]*Power Electrical Engineering, Ain Shams University, Cairo, Egypt.*

***Corresponding author**
Hesham Metwally, Power Mechanical Engineering, Egypt.

Submitted: 24 Oct 2022; **Accepted**: 04 Nov 2022: **Published**: 10 Nov 2022

Citation: *Metwally, H., Mahmoud, N. A. , Aboelsoud, W., Ezzat, M. (2022). Comprehensive analysis of PCM container construction effects PV panels thermal management. Adn Envi Was Mana Rec, 5(3), 326-338.*

Abstract

Current research aims to identify the finest phase change material container construction and tries to close the design gap for optimum photovoltaic panel thermal management. The phase change material is used as heat sink of photovoltaic panel and heat source for thermoelectric generator. The latent heat of phase change material maximizes the power generation from thermoelectric generator. The results show that the efficiency of the photovoltaic panel was enhanced by 3% and steady for ten hours. The photovoltaic panel electrical output power was enhanced by 25% under different weather conditions. The hybrid cooling system with capsules phase change material cavity shows a significant enhancement and stability in thermal system management, photovoltaic efficiency, and system output power.

Keywords: Photovoltaic Panel Temperature, Hybrid Cooling System, Thermal Management

Introduction

Hybrid cooling system overall performance is always higher than the passive and active cooling system performance when applicant separately, [1]. Some applications of the hybrid cooling system use the PV panel temperature as the TEG heat source. Other hybrid cooling systems use the PCM temperature as the TEG heat source. Heat removal by hybrid cooling systems is designing a system using both advantages of the passive and active cooling processes. The passive cooling system is the most common cooling technique according to the low running cost and high efficiency.

Many experiments were investigated the best phase change material (PCM) in the passive cooling process. Kandilli and Uzel [2] investigated the effect of paraffin wax, stearic acid, and natural zeolite on the energy efficiencies of PV thermal systems. As a result of the analyzes, the average energy efficiencies were estimated as 33%, 40%, 37% and 32% for paraffin, natural zeolite, stearic acid and conventional photovoltaic thermal (PVT) system, respectively. Shastry and Arunachala [3] investigated the effect of OM47 PCM, which enhanced thermal management by 11.1%. Hassan et al. [4] and Qasim et al. [5] investigated the cooling system enhancement using RT-35HC. They concluded that the cooling system enhanced by 23.9% and 13.3%, respectively. Moreover, the concentrated photovoltaic (CPV) implementation of mineral oil with graphene fillers decreased the CPV panel by 40 ºC, [6]. An experiment held by different PCM materials (organic RT50, inorganic C48. The results indicated that the PCM allowed power generation up to 30 % of the maximum power values in the unglazed case. In the glazed case, the power generation was enhanced by 25% with 12% thermal improvement, [7]. In another investigation performed in United Arab Emirates, the photovoltaic (PV) passive cooling process was investigated to determine its energy-saving and system efficiency throughout the year. PCM's cooling effect was low due to un melting at low ambient

NOMENCLATURE

A	Area	q_c	conduction heat transfer to PCM
C_p	Specific heat capacity	ΔT	Temperature difference
f	Liquid fraction of the PCM	T	Local temperature
G_{pv}	Solar intensity	T_{Sky}	Sky temperature
k	Thermal conductivity	T_{glass}	PV panel glass surface temperature
H	Enthalpy	T_{amb}	Ambient temperature
h	Heat convection coefficient	a	Absorption coefficient
L	Length	β_{ref}	Coefficient of PV efficiency
L_H	Latent PCM heat of fusion	β	Thermal expansion coefficient
q_v	Convection heat transfer	ρ	Material density
q_{rad}	Radiation heat transfer	η	Real PV conversion efficiency
Q_{in}	Absorbed heat by PV	ε	Seebeck coefficient
q_s	Absorbed Solar heat	ρ_o	Constant density of the flow

temperature and non-solidification at high ambient temperature, but the annual PV electrical generation increased by 5.9 %, [8].

Meanwhile, Klugmann and Wcisło [9] tested a mixed system of water and two separate PCMs to improve electrical parameters and decrease PV panel temperature. The passive cooling system on CPV was studied and subjected to a solar radiation strength of 670 W/m2. Simultaneously, the device was able to keep the average CPV cell temperature at around 5-6 ° C lower than usual. Another finding was that for CPV/PCM systems with horizontal Aluminum fins, the average temperature of PV cells was approximately 3°C lower than the CPV/PCM system's temperature without fins and can sustain for more than 5 hours [10]. Otherwise, a solar tracking CPV+PCM-T cooling system was investigated for identifying the passive cooling effects. The results found that the CPV+PCM-T cooling system increased the average electrical generation by 10 %, thermal efficiency by 5 %, and overall energy efficiency by 15 % compared to the CPV-T with thermal cooling [11]. Furthermore, paraffin wax RT42 was assessed with indoor experience using a light source of 1000 W/m2 to improve the building integration concentrated photovoltaic (BICPV) system's performance through thermal regulation. Results were showed a 7.7 % improvement in electrical efficiency and an average 3.8 °C decrease in module central temperature [12]. CPV+PCM cooling system was also investigated in severely hot ambient temperatures, [35]. For CPV+PCM cooling system, the evaluated CPV temperature was decreased by 28 °C [13]. In addition, the application of a water jacket around CPV+PCM increased the electrical efficiency to 17.7% [14].

Mathematical Analysis

PV panel is under many energy forms according to absorption of solar intensity and wind flows, creating an energy combination from radiation and convection [15].

$$Q = q - (q + q + q) \quad (1)$$

Where:

$$q = A\,h\,T - T \quad (2)$$

$$q = AG \quad (3)$$

$$q = \varepsilon\sigma A\,T - T \quad (4)$$

Where ε emissivity of the glass surface and σ is Stefan-Boltzmann constant. For the internal layers of the developed system are under conduction, when there is no linear momentum and no velocity gradient, the energy equation transfers [15] get

$$\frac{dT}{dt} = \frac{k}{\rho C_p}\left(\frac{\partial^2 T}{\partial x^2} + \frac{\partial^2 T}{\partial y^2} + \frac{\partial^2 T}{\partial z^2}\right) \quad (5)$$

PCM conduction heat depending on melting or solidification process so an additional term must be included in the energy equation [16], [17], and [18]. When f = 1 at liquid state and f = 0 at solid-state.

$$\rho\frac{dH}{dt} = \nabla.(k\nabla T) - L_H\frac{\partial f}{\partial t} \quad (6)$$

So, by Boussinesq expression the PCM density is described by equation Eq.(7).

$$\rho = \rho\,(1 - \beta\,\Delta T) \quad (7)$$

The evaluation of PV panel efficiency can be determined as per the next equation, [19].

$$\eta = \eta_{ref}\left(1 - \beta_{ref}\left(T_{glass} - T_{ref}\right) + \gamma\, log_{10}\left(\frac{G_{pv}}{1000}\right)\right) \quad (8)$$

Numerical Analysis

Hybrid cooling system model performed to use the latent heat in PCM to cool photovoltaic panel and generates power from thermoelectric generator, as seen in Figure 1.

a. Flat plate collector glass cover and silicon photovoltaic cell impeded in aluminum plate frame [20].

b. Aluminum container have thickness of 1mm and height of 30mm filled with PCM as seen in Figure 2. Organic paraffin wax is commonly used in nearly 90% of the studies [21] . Based on these criteria, a PCM RT-25 [22], [23] are selected with thermal characteristics as shown in TABLE 1. The PCM container con-

struction varied between four types of construction cavity volume (CV), Cavity Finned (CF), Cavity CHannel (CCH), and Cavity CaPsules (CCP) as shown in Table 2

c. Simple TEG products model with dimention of 40mmx 40mm x3.5mm [20].

d. Aluminum Water container with thickness of 1 mm and 8mm height have water flows under gravity at ambient temperature.

The PV model validated against the Zhou et al. [24] when the PCM model validated against Huang et al. [23]. Comparing the validation results found a variance of 0.18 K which is acceptable. The study performed for twenty-four hours with transient 12 hours solar intensity start from 6:00 AM to 6:00 PM in different weather condition. Fair weather condition with 880 W/m2 maximum irradiation flux at noon and sunny weather condition with 1250 W/m2 maximum irradiation flux at noon. The ambient is assumed steady at day with 301k and 292K at night when the forced convection coefficient *h* is 9.89 W/m2 K at 1 m/s wind speed [24].

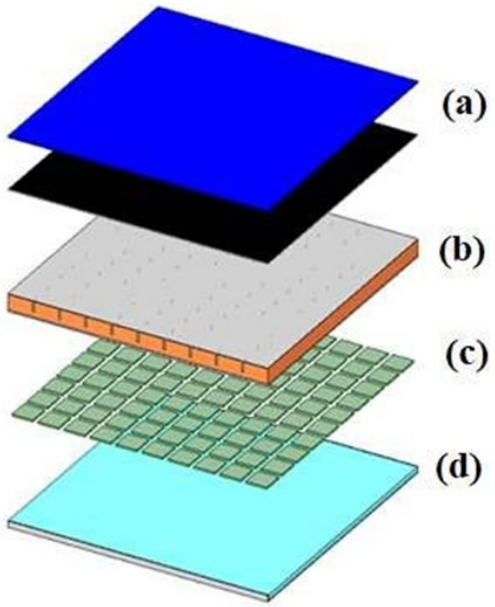

Figure 1:

Table 1: RT25 PCM Thermo Physical Properties [22].

Characteristics	Value
Density (solid) (g/ml)	0.88
Latent heat (kJ/kg)	230
Melting temperature (°C)	26
Solidification temp. (°C)	22
Specific heat (kJ/kg K)	2
Thermal conductivity (W/m K)	0.2
Viscosity (kg/m s)	0.0063
Volume expansion (%)	1.25

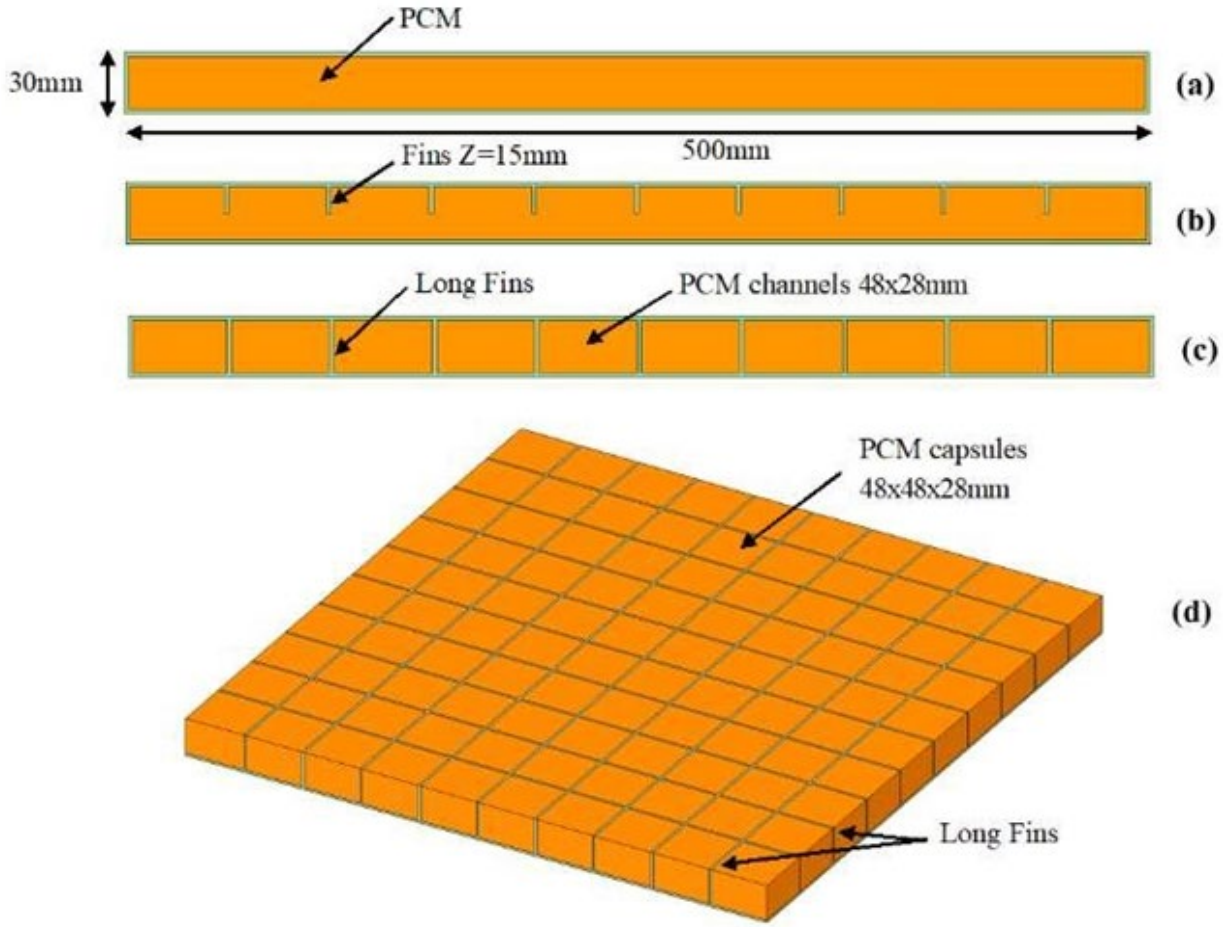

Figure 2: PCM Container Construction.

Table 2: PCM Container Construction.

Parameter	(a) CV	(b) CF	(c) CCH	(d) CCP
Material	Alumenium			
Thickness	2mm			
Fins	N/A	Yes	Yes	Yes
Fin Type	N/A	Short	Long	Long
Fin direction	N/A	H	H	H/V
Fin hieght	N/A	0.5 L	L	L

Results and Discussion

Results are compared with an uncooled PV panel, which is only under forced convection at ambient temperature. Comparison between different models at fair and sunny weather conditions offers a wide range of simulation data. Results compare the PV cell temperature, efficiency, and power generation enhancement. The peak PV cell temperature was 362K in sunny weather when the efficiency decreased to 11%. Otherwise, the peak PV panel temperature at fair weather was 342K when the efficiency decreased to 12.5%.

a. PV Panel Thermal Management Enhancement

Any PV cooling process aims to keep the PV cell temperature at a minimum. Figure 3 shows the PV cell temperature simulation results for 24 hours in both fair and sunny weather conditions. In fair weather, PCM cavity volume (CV) decreases the PV cell temperature to 315K at noon and 298K at sunset. Otherwise, PCM cavity finned (CF) enhances the PV cell cooling process by 8K at noon when the PV cell temperature is 298K at sunset. Meanwhile, applying a hybrid cooling system with PCM cavity channel (CCH) and PCM cavity capsules (CCP) controls the PV cell temperature under 297K for eight hours start from 9:00 AM to 5:00 PM. After sunset, the cooling system with CCH and CCP decreases the PV cell temperature until it reaches the ambient air temperature at sunrise. However, the cooling system with CV and CF keeps the PV cell temperature 6 K higher than other systems at sunrise according to stored latent heat in the PCM module.

In sunny weather, the cooling system with CF decreases the PV cell temperature to 327K at 2:00 PM when the CV decreases the PV cell temperature to 325K at 2:00 PM. Otherwise, the cooling system with CV and CF decreases the PV cell temperature to 298K at sunset. Meanwhile, the effect of the cooling system with CCH and CCP keeps the PV cell temperature at 300K from 11:00 AM to 3:00 PM with 14% temperature enhancement, and the PV cell temperature decreases to 295K at sunset. After sunset, the cooling system with CV and CF decreases the PV cell temperature to 297K when CCH and CCP system keeps the PV cell at 294K. The simulation results present a PV panel temperature drop by 30 °C in the application of PCM/CV and 45 °C in the application of PCM/CCP. Malvi et al. [25], Hassan et al. [4], Xu et al. [26], Maatallah et al. [27], and Preet et al. [28] results using the application of paraffin wax and water with an average temperature drop of 25 °C matches with current study results. The simulated hybrid cooling system enhances the PV cell temperature because of the low melting temperature PCM (RT25), the PCM cavity geometry CCP and CCH with long fins, and water convection with a steady temperature.

b. PV Panel Efficiency Enhancement

The PV panel efficiency is a major character in the estimation of the PV panel output power. The PV panel's high temperature decreases the PV panel efficiency. Figure 4 shows the PV panel efficiency enhancement from sunrise to sunset at both fair and sunny irradiation flux.

Simulation results under fair irradiation flux show that the PV panel efficiency is significantly enhanced by 3.5 % by applying a cooling system with CCH and CCP. The efficiency enhancement is continuing all day long. Application of the cooling system with CV and CF enhances the PV until 9:00 AM. The PV panel efficiency starts decreased below 15% up to sunset.

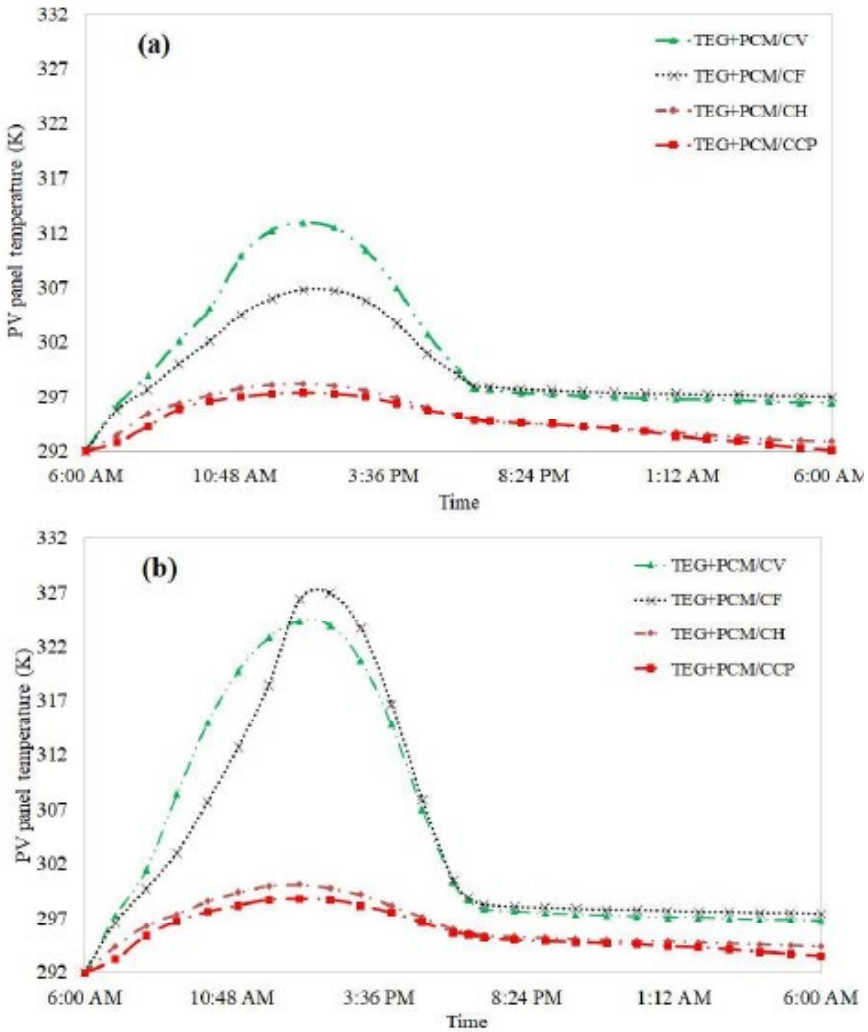

Figure 3: PV Panel Temperature at (a) Fair Weather and (b) Sunny Weather

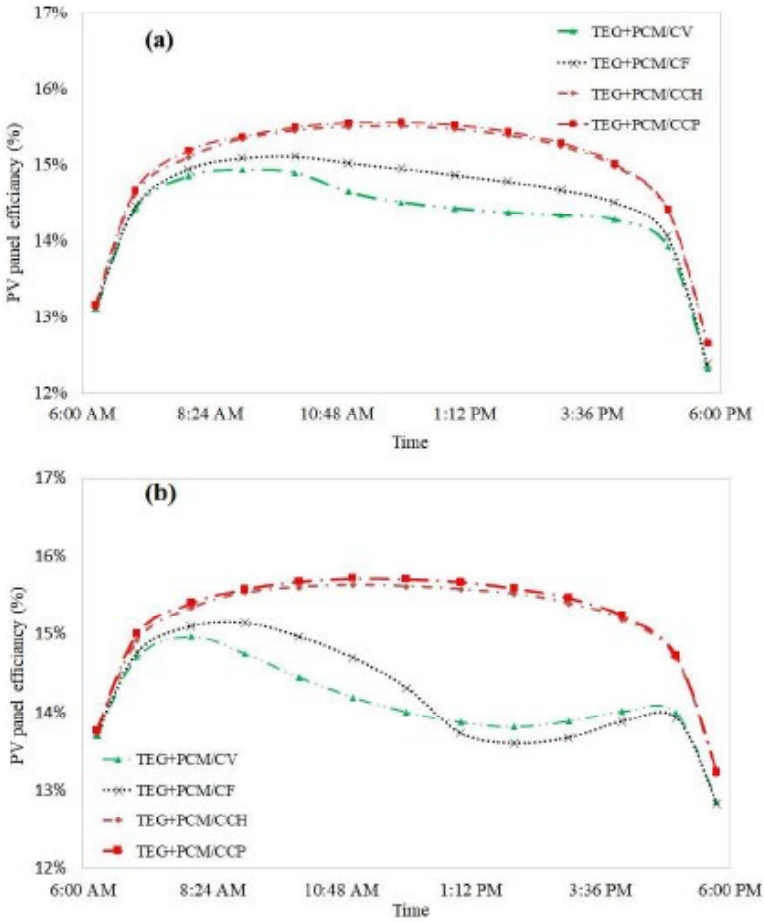

Figure 4: PV Panels Efficiency Enhancement at (a) Fair Weather and (b) Sunny Weather

Sunny irradiation flux increases the PV panel temperature, which decreases the PV panel efficiency. The cooling system with CV and CF increases the PV panel efficiency from sunrise to 9:00 AM and decreases until it reaches the minimum efficiency of 13.5% by 2:00 PM, then increases up to sunset. The cooling system with CCH and CCP keeps the PV panel efficiency above 15% and steady from sunrise to sunset.

c. Geometry Effect on Heat Transfer

The PCM Cavity geometry affects the amount of heat transfer rate and PCM melting process. Figure 5 and Figure 6 show the PCM liquid fraction in fair weather at noon and 4:00 PM, respectively. The liquid fraction of the cooling systems with CV and CF are in the solid stage at the bottom and complete liquid at contact with the PV panel. Otherwise, the cooling systems with CCH and CCP are in the solid stage according to the high thermal conductivity of aluminum fins. The long fins enhance the heat transfer rate between the PV panel and the TEG.

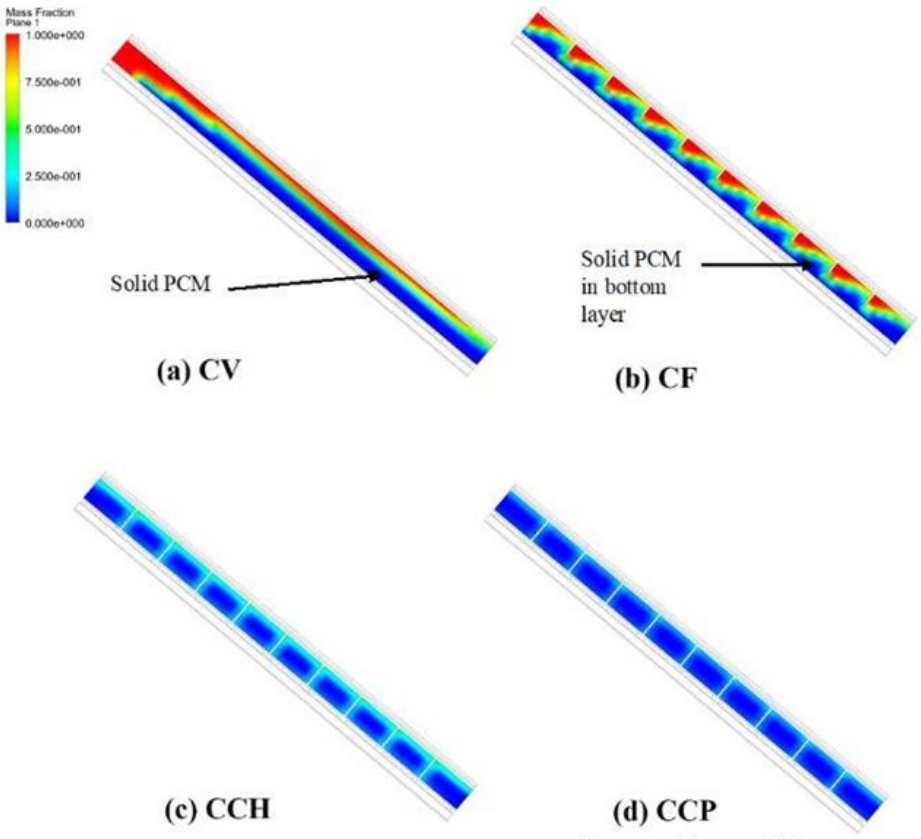

Table 5: Ultimate tensile strength of Zn-Co-Ni alloy coatings at different concentration of Co

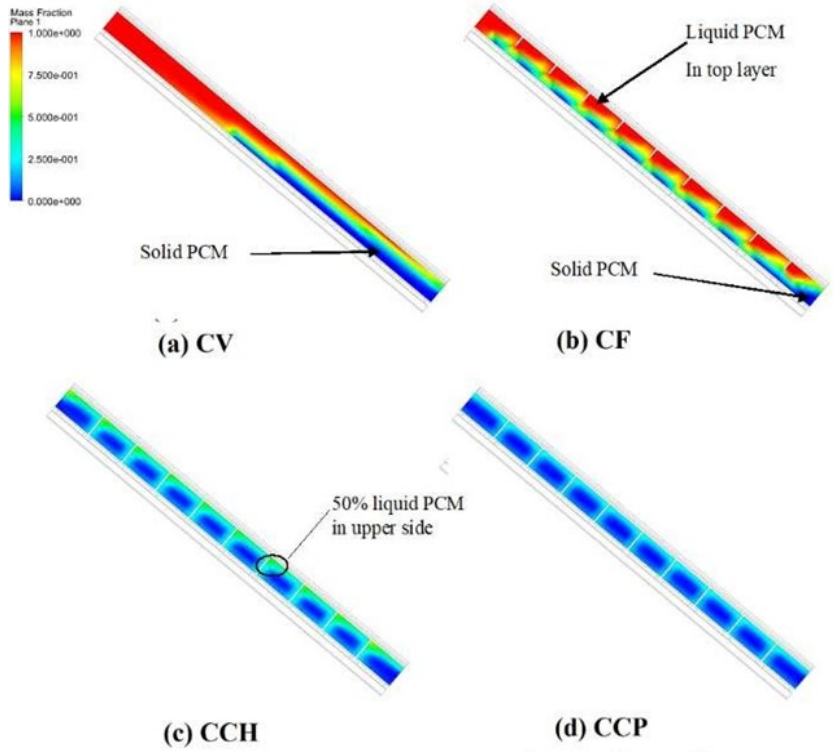

Figure 6: Fair Weather PCM Liquid Fraction at 4:00 PM

Figure 7 and Figure 8 show the PCM liquid fraction in sunny weather at noon and 4:00 PM, respectively. At noon, the PCM liquid fraction in the CV cavity is solid from the bottom and liquid from the top layer. Also, the CF cavity's PCM is melting completely from the top and upper sides when it is solid from the lower side. The PCM CCH cavity has a 50% liquid phase in the top layer and solid from the sides and bottom. In addition, the PCM in the CCP cavity is completely solid. At 4:00 PM, the CV and CF cavity's PCM is completely in the liquid phase, except a small amount on the lower side is still in a solid phase. The CCH cavity's PCM is on the liquid phase at the upper side and 50% solid at lower side and bottom. The CCP cavity's PCM is 50% liquid at the upper side and solid at the bottom and lower side.

Figure 7 and Figure 8 show the PCM liquid fraction in sunny weather at noon and 4:00 PM, respectively. At noon, the PCM liquid fraction in the CV cavity is solid from the bottom and liquid from the top layer. Also, the CF cavity's PCM is melting completely from the top and upper sides when it is solid from the lower side. The PCM CCH cavity has a 50% liquid phase in the top layer and solid from the sides and bottom. In addition, the PCM in the CCP cavity is completely solid. At 4:00 PM, the CV and CF cavity's PCM is completely in the liquid phase, except a small amount on the lower side is still in a solid phase. The CCH cavity's PCM is on the liquid phase at the upper side and 50% solid at lower side and bottom. The CCP cavity's PCM is 50% liquid at the upper side and solid at the bottom and lower side.

Figure 9 shows the PCM velocity contours in fair weather at noon and 4:00 PM. At noon, the CV cavity's PCM has a high velocity at the top layer and no motion at the bottom layer, so free convection heat transfer is applied at the top, and heat is transferred to TEG by conduction only. The CF cavity's PCM has no motion on all sides, so heat is transferred by conduction only. At 4:00 PM, the CV cavity's PCM has high velocity in the top and bottom layers when the CF cavity's PCM has no motion on all sides. Figure 10 shows the PCM velocity contours in sunny weather at noon and 4:00 PM. The CV cavity's PCM has a high velocity at the top and bottom layers. The CF cavity's PCM has a high velocity at the fin edge, so free convection is applied at the bottom layer. The CCH and CCP cavity's PCM are in the solid phase, so the heat transfers by conduction and the advantage of PCM free convection are not applied.

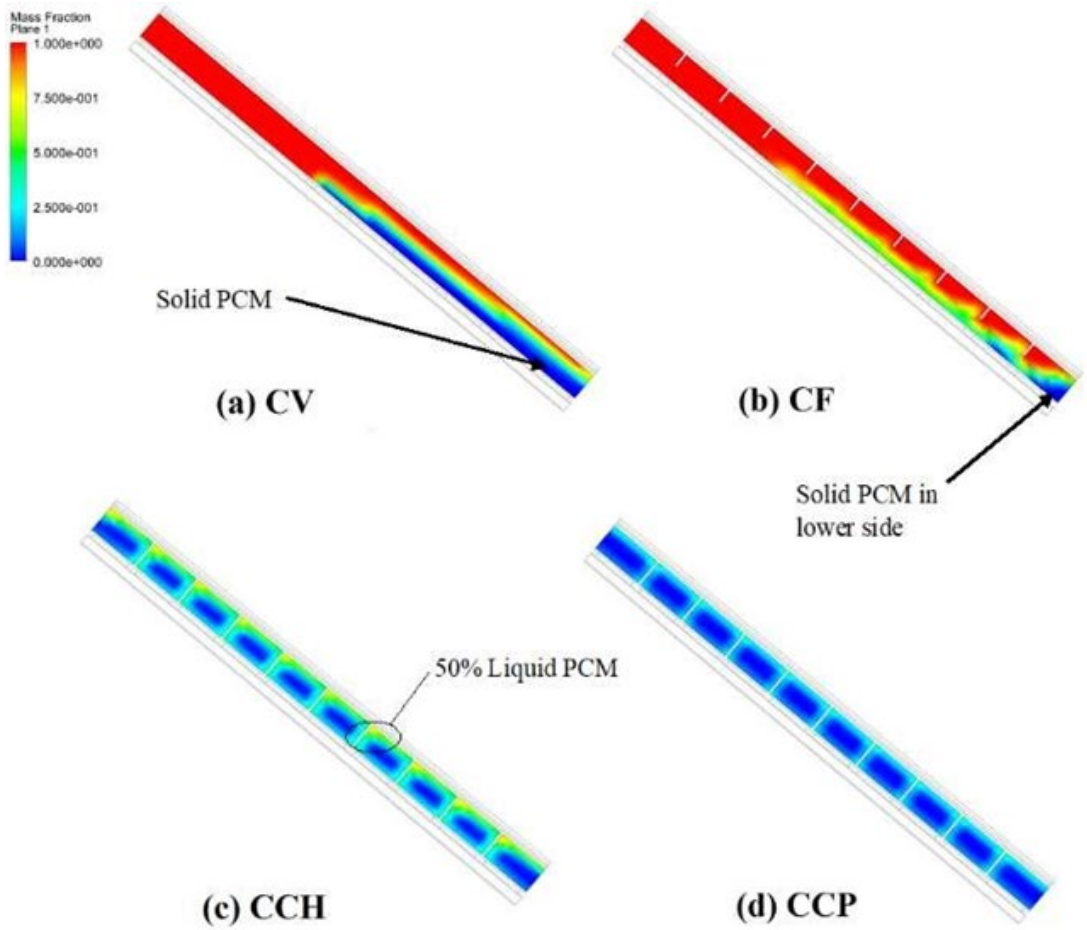

Figure 7: Sunny Weather PCM Liquid Fraction at noon.

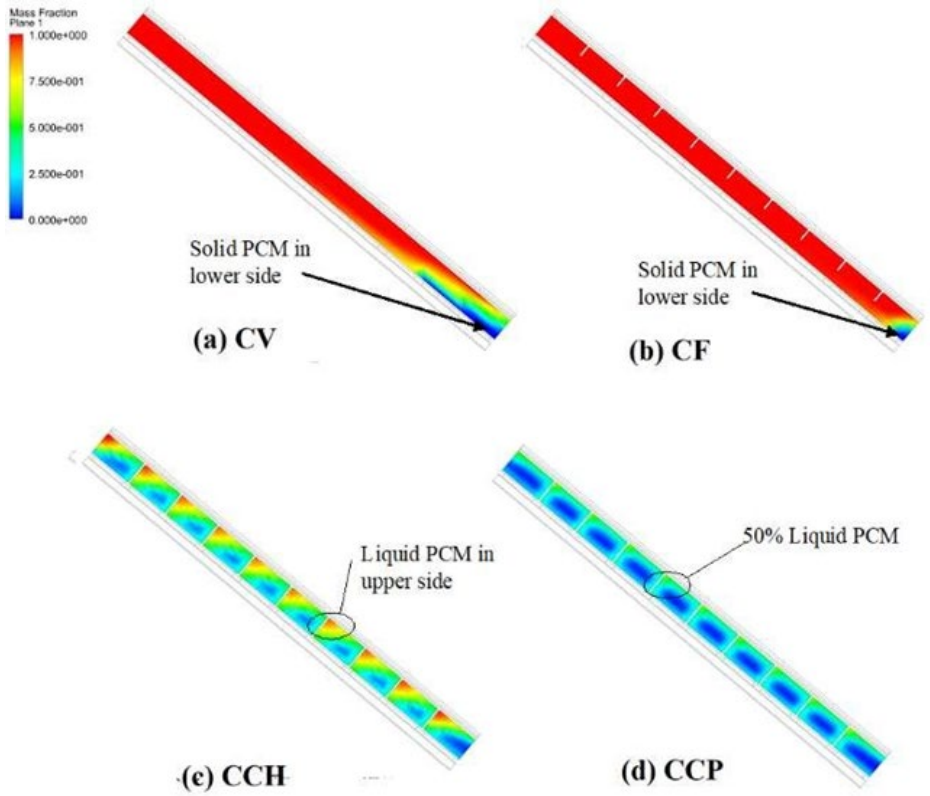

Figure 8: Sunny Weather PCM Liquid Fraction at 4:00 PM

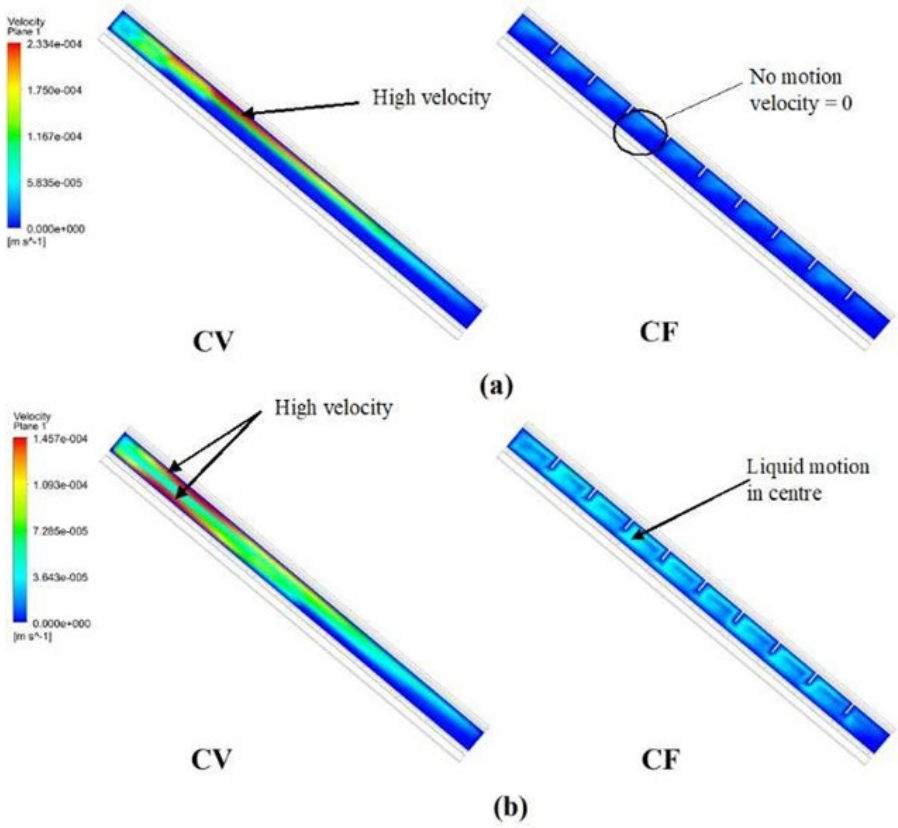

Figure 9: Fair Weather PCM Velocity at (a) noon and (b) 4:00 PM

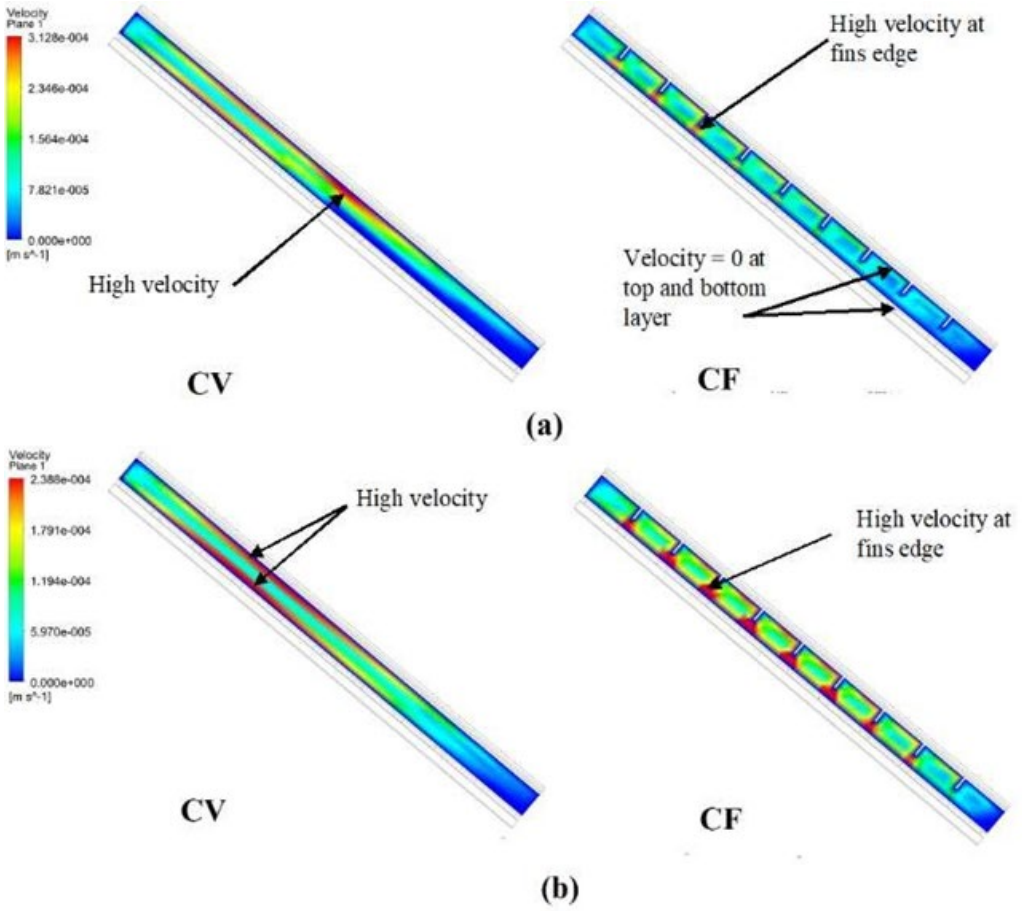

Figure 10: Sunny Weather PCM Velocity at (a) noon and (b) 4:00 PM

d. TEG Thermal Management

TEG temperature difference between the hot side temperature (TH) and cold side temperature (TC) significantly affects the cooling system's selection. Error! Reference source not found. shows the cooling system with CCH and CCP keeps the TEG temperature difference at 4.5K and 5.5K in fair and sunny weather, respectively. Otherwise, the CV and CF applications have the minimum TEG temperature difference in all weather conditions, providing a TEG temperature difference of 2K and 3.5K in fair and sunny weather, respectively. The effect of PCM thermal storage keeps a TEG temperature difference at night by 2K in CV and CF cavity's application. Otherwise, the TEG temperature difference decreases from sunset through the night until sunrise in the CCH and CCP cavity application.

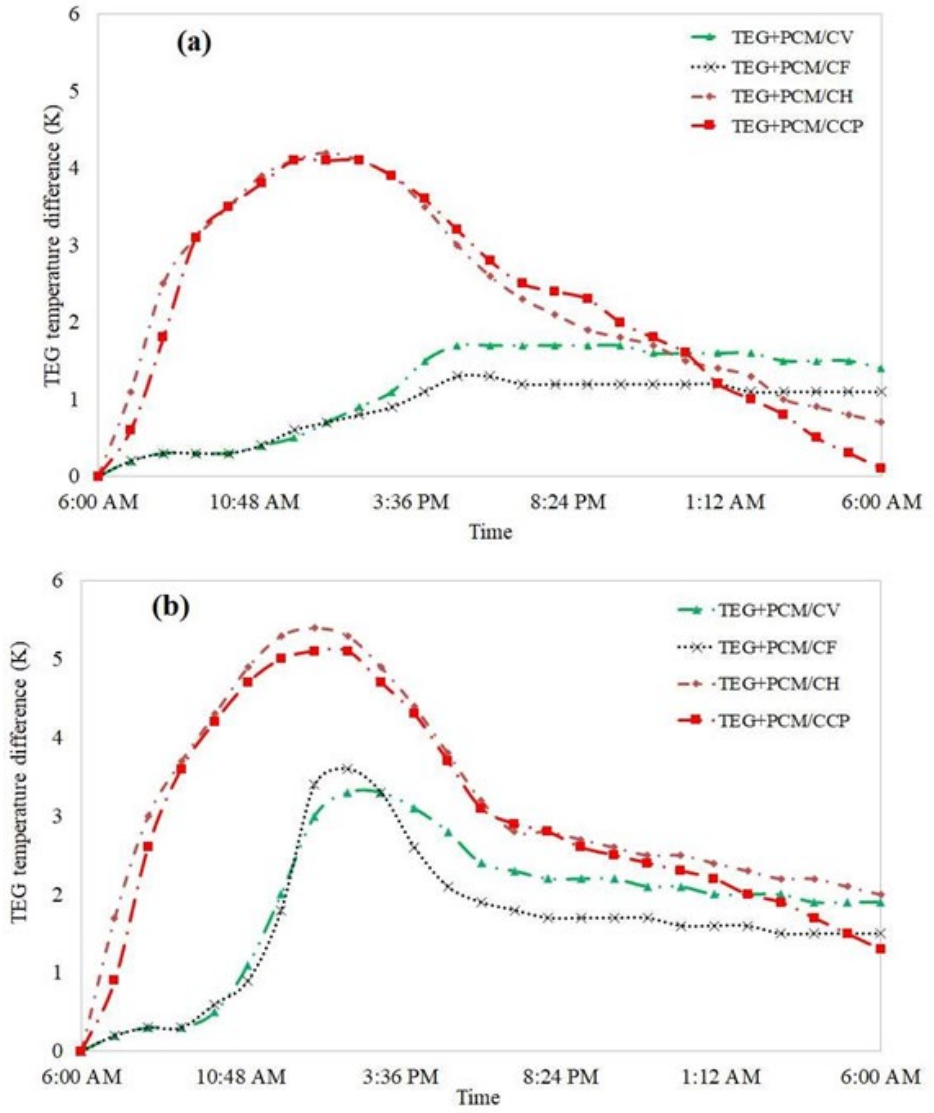

Figure 11: TEG Temperature Difference (TH-TC) at a) Fair-Weather b) Sunny Weather

Conclusions

The current study studied the photovoltaic panel's thermal management using the hybrid cooling system and the effect of PCM cavity geometry on the PV thermal management, PV efficiency, PV performance, and cooling system performance. The simulation was optimized under fair and sunny irradiation flux to present a wide range of results and system performance.

The PV hybrid cooling system uses the PCM thermal storage as a TEG heat source and water flow as a TEG heat sink.

The study is performed using four different PCM cavity geometry CV, CF, CCH, and CCP. The hybrid cooling process keeps the PV panel at a steady temperature for ten hours and increases the PV efficiency by 2.5% and 3.5% at fair and sunny weather, respectively. The cooling system CV and CCP decreases the PV temperature by 30 °C and 45 °C, respectively. The addition of short fins in CF geometry increases the PV temperature and decreases the PV efficiency.

The cooling system with CCH and CCP enhances the PV performance by 20% and 28% in fair weather. In sunny weather, the cooling system with CCH and CCP enhances the PV performance due to the PV panel efficiency enhancement. The TEG effect in the hybrid cooling system is maximized with CCH and CCP cavities geometry because of long aluminum fins. The CV and CF decrease the effect of TEG in system performance because of low PCM thermal conductivity and low free convection. The hybrid cooling system with PCM cavity capsules (CCP) significantly improves the cooling system performance and stability of PV temperature, PV efficiency, and PV performance.

Compliance with Ethical Standards

The corresponding author should be prepared to collect documentation of compliance with ethical standards and send, if requested, during peer review or after publication. the statement of compliance with standards of research involving animals and involving humans as subjects. all sources of financial support of each author and the team of authors.

Competing Interests

The authors did not receive support from any organization for the submitted work.

References

1. Shukla, A., Kant, K., Sharma, A., & Biwole, P. H. (2017). Cooling methodologies of photovoltaic module for enhancing electrical efficiency: A review. Solar Energy Materials and Solar Cells, 160, 275-286.
2. Kandilli, C., & Uzel, M. (2021). Exergoeconomic analysis of photovoltaic thermal systems based on phase change materials and natural zeolites for thermal management. Journal of thermal analysis and calorimetry, 145(3), 1373-1384.
3. Shastry, D. M. C., & Arunachala, U. C. (2020). Thermal management of photovoltaic module with metal matrix embedded PCM. Journal of Energy Storage, 28, 101312.
4. Hassan, A., Wahab, A., Qasim, M. A., Janjua, M. M., Ali, M. A., Ali, H. M., ... & Javaid, N. (2020). Thermal management and uniform temperature regulation of photovoltaic modules using hybrid phase change materials-nanofluids system. Renewable Energy, 145, 282-293.
5. Qasim, M. A., Ali, H. M., Khan, M. N., Arshad, N., Khaliq, D., Ali, Z., & Janjua, M. M. (2020). The effect of using hybrid phase change materials on thermal management of photovoltaic panels–an experimental study. Solar Energy, 209, 415-423.
6. Mahadevan, B. K., Naghibi, S., Kargar, F., & Balandin, A. A. (2019). Non-curing thermal interface materials with graphene fillers for thermal management of concentrated photovoltaic solar cells. C, 6(1), 2.
7. Simón-Allué, R., Guedea, I., Villén, R., & Brun, G. (2019). Experimental study of Phase Change Material influence on different models of Photovoltaic-Thermal collectors. Solar Energy, 190, 1-9.
8. Hasan, A., Sarwar, J., Alnoman, H., & Abdelbaqi, E. S. (2017). Yearly energy performance of a photovoltaic-phase change material (PV-PCM) system in hot climate. Solar Energy, 146, 417-429.
9. Klugmann-Radziemska, E., & Wcisło-Kucharek, P. (2017). Photovoltaic module temperature stabilization with the use of phase change materials. Solar Energy, 150, 538-545.
10. Lu, W., Liu, Z., Flor, J. F., Wu, Y., & Yang, M. (2018). Investigation on designed fins-enhanced phase change materials system for thermal management of a novel building integrated concentrating PV. Applied Energy, 225, 696-709.
11. Su, Y., Zhang, Y., & Shu, L. (2018). Experimental study of using phase change material cooling in a solar tracking concentrated photovoltaic-thermal system. Solar Energy, 159, 777-785.
12. Sharma, S., Tahir, A., Reddy, K. S., & Mallick, T. K. (2016). Performance enhancement of a Building-Integrated Concentrating Photovoltaic system using phase change material. Solar Energy Materials and Solar Cells, 149, 29-39.
13. Aoul, K. T., Hassan, A., Shah, A. H., & Riaz, H. (2018). Energy performance comparison of concentrated photovoltaic–Phase change material thermal (CPV-PCM/T) system with flat plate collector (FPC). Solar Energy, 176, 453-464.
14. Emam, M., & Ahmed, M. (2018). Performance analysis of a new concentrator photovoltaic system integrated with phase change material and water jacket. Solar Energy, 173, 1158-1172.
15. F. M. White, (1979). Fluid mechanics (seventh ed.).
16. Zivkovic, B., & Fujii, I. (2001). An analysis of isothermal phase change of phase change material within rectangular and cylindrical containers. Solar energy, 70(1), 51-61.
17. Voller, V. R., & Prakash, C. (1987). A fixed grid numerical modelling methodology for convection-diffusion mushy region phase-change problems. International journal of heat and mass transfer, 30(8), 1709-1719.
18. Brent, A. D., Voller, V. R., & Reid, K. T. J. (1988). Enthalpy-porosity technique for modeling convection-diffusion phase change: application to the melting of a pure metal. Numerical Heat Transfer, Part A Applications, 13(3), 297-318.
19. Smith, C. J., Forster, P. M., & Crook, R. (2014). Global analysis of photovoltaic energy output enhanced by phase change material cooling. Applied energy, 126, 21-28.
20. Metwally, H., Mahmoud, N. A., Aboelsoud, W., & Ezzat, M. (2021). Yearly performance of the photovoltaic active cooling system using the thermoelectric generator. Case Studies in Thermal Engineering, 27, 101252.
21. Ma, T., Li, Z., & Zhao, J. (2019). Photovoltaic panel integrated with phase change materials (PV-PCM): technology overview and materials selection. Renewable and Sustainable Energy Reviews, 116, 109406.
22. Huang, M. J., Eames, P. C., & Norton, B. (2006). Phase change materials for limiting temperature rise in building integrated photovoltaics. Solar energy, 80(9), 1121-1130.
23. Biwole, P. H., Eclache, P., & Kuznik, F. (2013). Phase-change materials to improve solar panel's performance. Energy and Buildings, 62, 59-67.
24. Zhou, J., Yi, Q., Wang, Y., & Ye, Z. (2015). Temperature distribution of photovoltaic module based on finite element simulation. Solar Energy, 111, 97-103.
25. Malvi, C. S., Dixon-Hardy, D. W., & Crook, R. (2011). Energy balance model of combined photovoltaic solar-thermal system incorporating phase change material. Solar Energy, 85(7), 1440-1446.
26. Xu, H., Zhang, C., Wang, N., Qu, Z., & Zhang, S. (2020). Experimental study on the performance of a solar photovoltaic/thermal system combined with phase change material. Solar Energy, 198, 202-211.
27. Maatallah, T., Zachariah, R., & Al-Amri, F. G. (2019). Exer-

go-economic analysis of a serpentine flow type water based photovoltaic thermal system with phase change material (PVT-PCM/water). Solar Energy, 193, 195-204.
28. Preet, S., Bhushan, B., & Mahajan, T. (2017). Experimental investigation of water based photovoltaic/thermal (PV/T) system with and without phase change material (PCM). Solar Energy, 155, 1104-1120.

Copyright: *©2022 Hesham Metwally. This is an open-access article distributed under the terms of the Creative Commons Attribution License, which permits unrestricted use, distribution, and reproduction in any medium, provided the original author and source are credited.*